Arabidopsis INOSITOL TRANSPORTER4 Mediates High-Affinity H^+ Symport of Myoinositol across the Plasma Membrane[1]

Sabine Schneider, Alexander Schneidereit, Kai R. Konrad, Mohammad-Reza Hajirezaei, Monika Gramann, Rainer Hedrich, and Norbert Sauer*

Molekulare Pflanzenphysiologie, Friedrich-Alexander-Universität Erlangen-Nürnberg, D–91058 Erlangen, Germany (S.S., A.S., M.G., N.S.); Julius-von-Sachs-Institut für Biowissenschaften, Molekulare Pflanzenphysiologie und Biophysik, D–97082 Wuerzburg, Germany (K.R.K., R.H.); and Institut für Pflanzengenetik und Kulturpflanzenforschung, D–06466 Gatersleben, Germany (M.-R.H.)

Four genes of the Arabidopsis (*Arabidopsis thaliana*) monosaccharide transporter-like superfamily share significant homology with transporter genes previously identified in the common ice plant (*Mesembryanthemum crystallinum*), a model system for studies on salt tolerance of higher plants. These ice plant transporters had been discussed as tonoplast proteins catalyzing the inositol-dependent efflux of Na^+ ions from vacuoles. The subcellular localization and the physiological role of the homologous proteins in the glycophyte Arabidopsis were unclear. Here we describe *Arabidopsis INOSITOL TRANSPORTER4* (*AtINT4*), the first member of this subgroup of Arabidopsis monosaccharide transporter-like transporters. Functional analyses of the protein in yeast (*Saccharomyces cerevisiae*) and *Xenopus laevis* oocytes characterize this protein as a highly specific H^+ symporter for myoinositol. These activities and analyses of the subcellular localization of an AtINT4 fusion protein in Arabidopsis and tobacco (*Nicotiana tabacum*) reveal that AtINT4 is located in the plasma membrane. *AtINT4* promoter-reporter gene plants demonstrate that *AtINT4* is strongly expressed in Arabidopsis pollen and phloem companion cells. The potential physiological role of AtINT4 is discussed.

In higher plants, cyclic polyol myoinositol and derivatives of this compound play important roles in several metabolic pathways and under several physiological conditions. For example, myoinositol represents a precursor in the synthesis of the nucleotide sugar UDP-GlcUA, which in turn is used for the synthesis of GalUA, Xyl, apiose, and Ara, important residues of plant cell wall polymers (Loewus and Murthy, 2000; Kanter et al., 2005). As an integral part of galactinol, myoinositol acts as a carrier of activated Gal that is eventually transferred to Suc, yielding raffinose and its longer derivatives (Kandler and Hopf, 1982). Myoinositol has also been discussed as an initial substrate in a newly described biosynthetic route for L-ascorbic acid synthesis (Lorence et al., 2004). Moreover, phytic acid (myoinositol-1,2,3,4,5,6-hexakisphosphate), the product of inositol phosphorylation (Shi et al., 2005), represents a storage form for both inositol and phosphorus, is involved in mineral storage, and may even represent a cellular energy currency (Raboy, 2003). Finally, as a component in glycosylphosphatidylinositol-membrane anchors (Schultz et al., 1998) and especially as a component of phospholipids (Lehle, 1990), inositol is involved not only in providing the structural basis for membranes and membrane-attached proteins, but also in several signaling pathways.

In many plants, the concentration of myoinositol is massively increased in response to salt stress. The reason is that compounds such as myoinositol, pinitol, or ononitol, can be accumulated to high concentrations as osmolytes (Thomas and Bohnert, 1993; Sheveleva et al., 1997; Nelson et al., 1998). In other species, however (e.g. in Arabidopsis [*Arabidopsis thaliana*]), salt treatment, but also drought stress or cold stress, results in enhanced synthesis of raffinose and increased myoinositol levels reflect an increased demand for galactinol (Taji et al., 2002).

Despite these essential functions of myoinositol in plant biology and despite the profound knowledge of myoinositol metabolism in plants, little is known about the partitioning of this molecule between different cells, tissues, or subcellular compartments. Nelson and coworkers (1999) performed the first analysis of higher plant myoinositol transport in the common ice plant (*Mesembryanthemum crystallinum*). In salt-stressed ice plants, these authors observed increased phloem transport of myoinositol from leaves to roots

[1] This work was supported by the Deutsche Forschungsgemeinschaft (grant to N.S. [Arabidopsis Functional Genomics Network; Sa 382/13-1]).

* Corresponding author; e-mail nsauer@biologie.uni-erlangen.de; fax 49–9131–8528751.

The author responsible for distribution of materials integral to the findings presented in this article in accordance with the policy described in the Instructions for Authors (www.plantphysiol.org) is: Norbert Sauer (nsauer@biologie.uni-erlangen.de).

Article, publication date, and citation information can be found at www.plantphysiol.org/cgi/doi/10.1104/pp.106.077123.

and simultaneously increased sodium and myoinositol transport from roots to leaves in the xylem. Independent analyses with exogenously supplied myoinositol showed a similar increase of Na^+ flux from the roots to the leaves and, based on this correlation, the authors speculated that the uptake of Na^+ ions into the xylem might be coupled to the uptake of myoinositol. Furthermore, they suggested that this capacity to couple Na^+ and myoinositol fluxes might be a specific property of salt-tolerant plants that is missing in glycophytes (Nelson et al., 1999).

The first cDNAs of putative plant myoinositol transporters were cloned from ice plant. One of these cDNAs (*Mesembryanthemum INOSITOL TRANSPORTER1* [*MITR1*]) was expressed in a mutant line of yeast (*Saccharomyces cerevisiae*; Chauhan et al., 2000) harboring defects in the yeast myoinositol transporter gene *ITR1* and in the inositol biosynthetic gene *INO1* (Nikawa et al., 1991). In fact, *MITR1*-expressing yeast cells were able to grow on lower extracellular concentrations of myoinositol than control cells. Moreover, these cells showed enhanced growth rates in the presence of NaCl (Chauhan et al., 2000). In combination with other results, this was interpreted as evidence for Na^+-coupled myoinositol transport (Chauhan et al., 2000). Anti-MITR1 antibodies identified the protein in a tonoplast fraction from Mesembryanthemum, and MITR1 was described as a vacuolar myoinositol-Na^+ symporter.

Only recently, a plasma membrane-localized transporter from Arabidopsis was shown to mediate the uptake of a wide range of different substrates, including monosaccharides (pentoses and hexoses), linear polyols of different chain lengths (3–6 carbons), and myoinositol (AtPLT5; Klepek et al., 2005). The AtPLT5 protein was studied in bakers' yeast and *Xenopus laevis* oocytes and both expression systems characterized the protein as an H^+ symporter (Klepek et al., 2005). MITR1 and AtPLT5 are members of two different subfamilies of the monosaccharide transporter-like (MST-like) superfamily of plant transporters. Whereas direct proof for the activity of MITR1 or related plant transporters is lacking, polyol transporter (PLT)-type proteins were studied successfully in several plant species (Noiraud et al., 2001; Gao et al., 2003; Ramsperger-Gleixner et al., 2004; Watari et al., 2004; Klepek et al., 2005). Evidence for myoinositol transport capacity of PLT-type transporters has not only been obtained for AtPLT5 (Klepek et al., 2005), but also for sorbitol transporters from apple (*Malus domesticus*) that are inhibited by myoinositol (Watari et al., 2004). However, there was no evidence that myoinositol might be the physiological substrate for any of these transporters and, therefore, the search for plasma membrane-localized myoinositol transporters continued.

In this study, we concentrated on the analysis of one of four Arabidopsis proteins sharing homology with MITR1. These proteins represent an independent subgroup within the Arabidopsis MST-like superfamily. All previously characterized proteins of this superfamily were shown to be H^+ symporters (AtSTP1 [Sauer et al., 1990]; AtPLT5 [Klepek et al., 2005]). We were interested to see whether the members of this previously uncharacterized subfamily do indeed transport myoinositol, whether they are located in the vacuole, and whether they transport their substrates together with Na^+ ions.

Here we present the cloning, functional characterization, tissue-specific expression, and subcellular localization of Arabidopsis INOSITOL TRANSPORTER4 (AtINT4). AtINT4 is one of four highly homologous proteins from Arabidopsis and transports myoinositol with high specificity. AtINT4 is localized in the plasma membrane and expression of *AtINT4* cDNA in both yeast and Xenopus independently confirmed that it transports myoinositol with high affinity and high specificity. Xenopus expression data show that AtINT4 is an H^+ symporter. The physiological role of the protein was studied with *AtINT4* promoter-β-glucuronidase (*GUS*) and with *AtINT4* promoter-green fluorescent protein (*GFP*) reporter lines with immunohistochemical techniques and in analyses of a T-DNA insertion line.

RESULTS

Cloning of *AtINT* cDNAs

In silico analyses of the Arabidopsis genome identified four open reading frames (ORFs) for putative transporters sharing homology with MITR1 (accession no. AF280431) and MITR2 (accession no. AF280432) from ice plant (Chauhan et al., 2000; 52.2% to 72.7% sequence identity on the protein level) and with ScITR1 from yeast (Robinson et al., 1996; 35.8% to 37.1% sequence identity on the protein level). Because the function of the plant transporters had been predicted from growth analyses of transgenic yeast (Chauhan et al., 2000), we decided to perform detailed analyses for one of the Arabidopsis proteins in different expression systems. To this end, cDNAs covering the entire ORFs were generated by reverse transcription-PCR from whole-plant mRNA and sequenced. The corresponding genes were named *AtINTs* (At2g43330, *AtINT1*; At1g30220, *AtINT2*; At2g35740, *AtINT3*; and At4g16480, *AtINT4*).

The obtained cDNA sequences confirmed the predicted protein sequences of AtINT2 (580 amino acids) and AtINT4 (582 amino acids). For AtINT1, two different ORFs had been predicted, one with 509 amino acids (accession no. NP_850393) and one with 521 amino acids (accession no. AAB64332). Our analyses confirmed the shorter ORF for an AtINT1 protein with 509 amino acids. We were not able to amplify a cDNA for *AtINT3* that is predicted to encode a protein of 580 amino acids (accession no. NP_181117) that is similar to AtINT2 and AtINT4 with 60.4% and 63.4% identical amino acids. The obtained cDNA sequences for *AtINT1*, *AtINT2*, and *AtINT4* were submitted to the EMBL Nucleotide Sequence Database (accession nos.

AtINT1, AJ973175; *AtINT2*, AJ973176; and *AtINT4*, AJ973178). Hydropathy analyses of the deduced protein sequences predicted 12 transmembrane helices for all AtINT proteins (data not shown) and sequence comparisons with other transporters characterized them as a separate group within the Arabidopsis MST-like superfamily (http://www.arabidopsis.org/info/genefamily/genefamily.html).

Figure 1 presents a phylogenetic tree based on the experimentally confirmed protein sequences of AtINT1, AtINT2, and AtINT4 and on the predicted sequence of AtINT3 (NP_181117). AtINT4 is closely related to ice plant MITR proteins. One of the AtINT proteins (AtINT1) is much smaller than all other proteins in Figure 1 (509 amino acids versus 580 to 584 amino acids). This difference results from an 80-amino acid fragment that is missing in the loop between the predicted transmembrane helices IX and X of AtINT1. Hydropathy analyses (data not shown) predict this loop to be opposite the N and C termini (i.e. outside the cell in a plasma membrane transporter or inside the vacuole in a vacuolar transporter). There are two consensus sequences for *N*-glycosylation in AtINT4 (Asn_{312}-Lys_{313}-Thr_{314} and Asn_{385}-Ala_{386}-Thr_{387}). Consensus sequences are located between predicted transmembrane helices VII and VIII or in the large loop between predicted transmembrane helices IX and X. Thus, these Asn residues do face the lumen of the endoplasmic reticulum and may be *N*-glycosylated during protein biosynthesis. Both glycosylation sites are conserved in AtINT2 and AtINT3, but are missing from AtINT1, which has no consensus sequence for *N*-glycosylation.

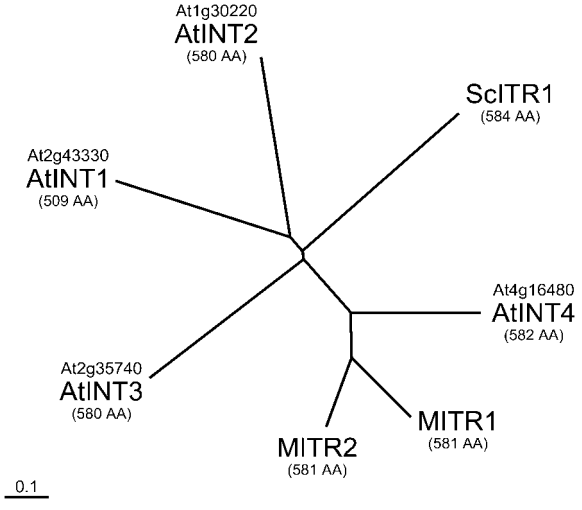

Figure 1. Phylogenetic tree of the AtINT family from Arabidopsis. The deduced sequences of the four Arabidopsis AtINTs were aligned with the program ClustalX (Thompson et al., 1997) and an unrooted tree was calculated using TreeViewX software (Page, 1996). The protein names and the Munich Information Center for Protein Sequences numbers of the corresponding genes are given. The lengths of the proteins (amino acids [AA]) were confirmed by sequencing the corresponding cDNAs for AtINT1, AtINT2, and AtINT4. The length of the AtINT3 protein was deduced from the genomic sequence (accession nos. are given in the text). The protein sequences of the homologous inositol transporters from yeast (ScITR1, YDR497C) and of the published Na^+/inositol symporters MITR1 (accession no. AF280431) and MITR2 (accession no. AF280432) from Mesembryanthemum were included.

The calculated pI (IP) of AtINT4 is 8.70. This value is similar to the values for AtINT2 (IP = 8.25) and AtINT3 (IP = 7.74) and different from the value for AtINT1 (IP = 5.05). The IP values of AtINT2, AtINT3, and AtINT4 also resemble the quite basic IP values of numerous plasma membrane transporters (e.g. AtSTP1 [Sauer et al., 1990; IP = 9.49]; AtSUC2 [Sauer and Stolz, 1994; IP = 9.55]; and AtPLT5 [Klepek et al., 2005; IP = 10.39]).

Expression of the *AtINT4* cDNA in Yeast

To determine the functional properties of this new group of Arabidopsis transporters, we cloned the cDNA of *AtINT4*, the first full-length clone obtained, into the unique *Eco*RI site of the yeast expression vector NEV-E-Leu, which is a modification of NEV-E (Sauer and Stolz, 1994), where the *URA3* selection marker has been replaced by *LEU2*. The resulting plasmids harbor the *AtINT4* cDNA in sense (pSS49sense) or antisense (pSS49antisense) orientation and were used to transform yeast strain D458-1B (Nikawa et al., 1991). This strain carries mutations in the inositol transporter (*ITR1*) and *INO1* inositol-1-P (*INO1*) synthase genes and can grow only on high extracellular concentrations of myoinositol.

The resulting yeast strains SSY33 (sense *AtINT4*) and SSY34 (antisense *AtINT4*) were grown on petri plates containing low (2 μg/mL) or high (20 μg/mL) concentrations of myoinositol to study the possible complementation of the mutations in myoinositol uptake and biosynthesis. Figure 2 shows that SSY33 cells had regained the capacity to grow on low myoinositol, whereas hardly any growth was seen for control strains (SSY35 with the empty vector or SSY34 with the antisense plasmid) on the same medium. This was evidence that *AtINT4* does encode a myoinositol transporter.

Chauhan et al. (2000) had used the same yeast mutant for complementation with MITR1 and got a similar result. In addition, these authors observed a growth-accelerating effect in the presence of 10 mM NaCl, and this was one of the observations that finally led to the interpretation that MITR1 is a Na^+/inositol symporter. We tested whether this is also seen in *AtINT4*-expressing yeast cells (Fig. 2). In fact, SSY33 cells do grow significantly better on plates supplemented with 10 mM NaCl.

With SSY33, we tried to determine the K_m value, substrate specificity, and sensitivity of AtINT4 to uncouplers. However, transport rates determined with ^{3}H-labeled myoinositol were too low to allow such analyses (data not shown). Apparently, the amount of AtINT4 protein in the yeast plasma membrane is sufficiently high for complementation, but not high

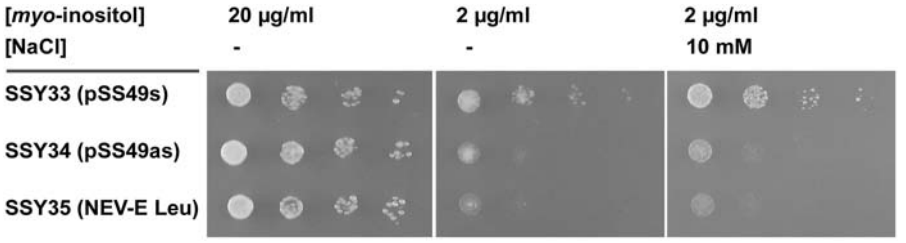

Figure 2. Complementation of the *itr1* mutation by *AtINT4* expression in the yeast strain D458-1B. Growth of the yeast strains SSY33 (D458-1B with *AtINT4* cDNA in sense orientation), SSY34 (D458-1B with *AtINT4* cDNA in antisense orientation), and SSY35 (D458-1B with the empty shuttle vector NEV-E-Leu) was analyzed on petri plates (minimal medium) supplemented with the indicated concentrations of myoinositol and NaCl. Whereas all three strains were able to grow on high myoinositol (20 μg/mL), only the *AtINT4*-expressing strain was able to grow on low myoinositol. Growth on low myoinositol was enhanced in the presence of 10 mM NaCl.

enough to allow direct measurement of radiolabeled substrates. In fact, when an *AtINT4-GFP* fusion was expressed in baker's yeast, most of the GFP fluorescence remained inside the cells, most likely in the endoplasmic reticulum (data not shown).

For further analyses of the AtINT4 transport properties, we had to use a different expression system.

Expression of the *AtINT4* cDNA in *X. laevis* Oocytes

X. laevis oocytes are a perfect tool for analyses of electrogenic plant plasma membrane transporters (Aoshima et al., 1993; Boorer et al., 1996) and have only recently been used for the successful expression of the plasma membrane H^+ symporter AtPLT5 (Klepek et al., 2005; Reinders et al., 2005). Due to the complementation data obtained with the yeast system, which suggested plasma membrane localization also for AtINT4, we decided to analyze AtINT4 in this expression system. To this end, *AtINT4* cDNA was cloned into pDK148 (Jespersen et al., 2002), yielding pMG001. cRNA was transcribed from the T_7 promoter of pMG001 and injected into oocytes, which were analyzed for inward currents resulting from the cotransport of cations with potential substrates.

Figure 3A shows a recording of inward currents in the presence of the different substrates tested. Analyses were performed with 10 mM solutions of myoinositol, Suc, sorbitol, Glc, or Fru at an extracellular pH of 5.5. Only myoinositol gave a strong inward current. No significant currents were obtained with any of the other compounds. This confirms and extends the results obtained in the yeast complementation analysis, showing that AtINT4 does mediate import of myoinositol into injected Xenopus oocytes. Furthermore, the obtained inward currents demonstrate that a positive charge is symported with myoinositol, confirming that AtINT4-driven transport is energy dependent. Finally, this result shows that, in contrast to the previously described AtPLT5 transporter, which has low substrate specificity (monosaccharides, linear polyols, and even myoinositol), AtINT4 seems to be highly specific for myoinositol. In addition to the compounds tested in Figure 3A, no significant currents were obtained by mannitol, xylitol, Xyl, Gal, Ara, erythritol, inositol-6-P, Rib, glycerol, or gluconate (each $n \geq 4$; data not shown). Only pinitol, a methylated derivative of myoinositol, is also transported by AtINT4, although at lower rates (28.4% $\pm$ 2.1% [$n = 12$]) than myoinositol (Fig. 3A, inset).

The identity of the cotransported ion was determined by replacing individual ions in the extracellular solution. There was no difference between the currents elicited with 95 mM KCl/0 mM NaCl or with 95 mM NaCl/0 mM KCl (data not shown); also, the simultaneous replacement of K^+ and Na^+ by *N*-methylglucamine$^+$ (NMG-Cl) had no effect on the resulting inward currents (Fig. 3B; $n = 9$). This demonstrates that protons are cotransported ions and that AtINT4 is a myoinositol/H^+ symporter.

Figure 3C shows one of 10 independent measurements where the inward H^+ currents elicited by myoinositol decreased with increasing extracellular pH. Similar pH dependence had been described for the AtPLT5 PLT, which has only recently been characterized as an H^+ symporter (Klepek et al., 2005).

A typical substrate dependence of AtINT4 for myoinositol is shown in Figure 3D and the corresponding Michaelis-Menten kinetics are presented in Figure 3E. K_m values were determined at three different membrane potentials (−90 mV, −40 mV, and 0 mV) at an extracellular pH of 5.5. Unexpectedly, there was no difference at these different membrane potentials and an average K_m of 0.24 $\pm$ 0.01 mM could thus be calculated from 10 independent analyses (Fig. 3E). This value is significantly lower than the K_m for myoinositol determined for AtPLT5 in Xenopus oocytes (3.5 $\pm$ 0.3 mM; Klepek et al., 2005), indicating that AtINT4 is a high-affinity transporter for myoinositol.

Analysis of *AtINT4* Expression in *AtINT4* Promoter-*GUS* and *AtINT4* Promoter-*GFP* Plants

For analysis of the tissue specificity of *AtINT4* expression, we generated and analyzed *AtINT4* promoter-*GUS* and *AtINT4* promoter-*GFP* plants. A 1,518-bp

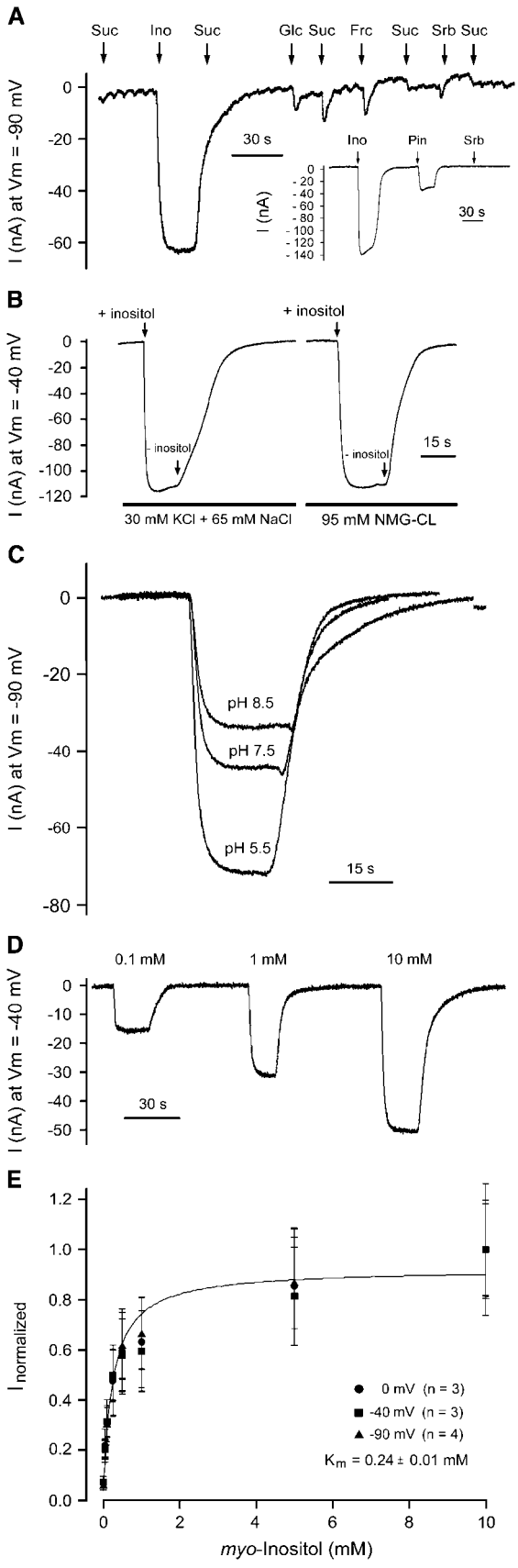

promoter fragment was used to drive the expression of *GUS* or *GFP* in plants that had been selected for gluphosinate resistance after transformation with the plasmids pLEX110 (*AtINT4* promoter *GUS*) or pLEX164 (*AtINT4* promoter *GFP*). We obtained numerous *GUS*- or *GFP*-expressing transformants and analyzed 24 independent *AtINT4* promoter-*GUS* lines and 24 independent *AtINT4* promoter-*GFP* lines.

Based on microarray analyses, strong and specific expression of *AtINT4* had been predicted in Arabidopsis stamina (https://www.genevestigator.ethz.ch). Our *AtINT4* promoter-*GUS* and *AtINT4* promoter-*GFP* plants confirmed this prediction (Fig. 4, A, G, and H), and more detailed analyses revealed that the strong GUS-histochemical staining and GFP fluorescence in anthers is restricted to pollen (Fig. 4, B and H). The well-known autofluorescence of Arabidopsis pollen that is detected under the same conditions (data not shown) was much weaker and had a clearly distinguishable color (yellowish).

In addition to the promoter activity in pollen, we also observed GUS staining and GFP fluorescence in the leaves of these plants (Fig. 4, C–E and I). This leaf-specific promoter activity was restricted to the vascular tissue and absent from the mesophyll (Fig. 4, D and I). It was also seen in the vascular tissues of cotyledons, hypocotyls, and roots (Fig. 4, C and E). This vascular-specific *AtINT4* expression in leaves depended strongly on the developmental stage. No promoter activity was found in young sink leaves (Fig. 4, C and E, red arrows), whereas strong expression was seen in all veins of fully developed source leaves (Fig. 4C). During the sink-to-source transition (transition leaves), *AtINT4* expression started in the very tips of the leaves (Fig. 4, C and E, black arrows) and

Figure 3. Substrate specificity and kinetic properties of AtINT4 as determined in *X. laevis* oocytes injected with *AtINT4* cRNA. A, AtINT4 mediates inward currents in response to myoinositol, but not to any of the other sugars or sugar alcohols tested. An exception is pinitol, a methylated derivative of myoinositol, which does elicit a significantly smaller current than myoinositol (inset). Ino, Myoinositol; Frc, Fru; Srb, sorbitol; Pin, pinitol (all 10 mM). Currents were recorded at pH 5.5 and a membrane potential of −90 mV. B, The nature of the cotransported ion was identified by the simultaneous replacement of 30 mM KCl and 65 mM NaCl in the bath solution with 95 mM NMG-Cl. This result demonstrates that H^+, but neither Na^+ nor K^+, is cotransported with myoinositol. C, Similar analyses of myoinositol-dependent H^+ currents as in A were performed at three different pH values as indicated. Currents were recorded at a membrane potential of −90 mV. D, Myoinositol-dependent inward H^+ currents were determined at increasing myoinositol concentrations (0.1 mM, 1 mM, and 10 mM) at a membrane potential of −40 mV and a pH of 5.5. E, Dependency of the myoinositol concentration of AtINT4-mediated H^+ currents reveals its high affinity to the substrate. Saturating curve for myoinositol-induced H^+ currents. Normalized currents (±SE) determined at membrane potentials of −90 mV (n = 4), −40 mV (n = 3), and 0 mV (n = 3) were plotted against the substrate concentration. Data were fitted with Michaelis-Menten-type kinetics and show a K_m value of 0.24 ± 0.01 mM for the membrane voltages used. Results ± SE are presented.

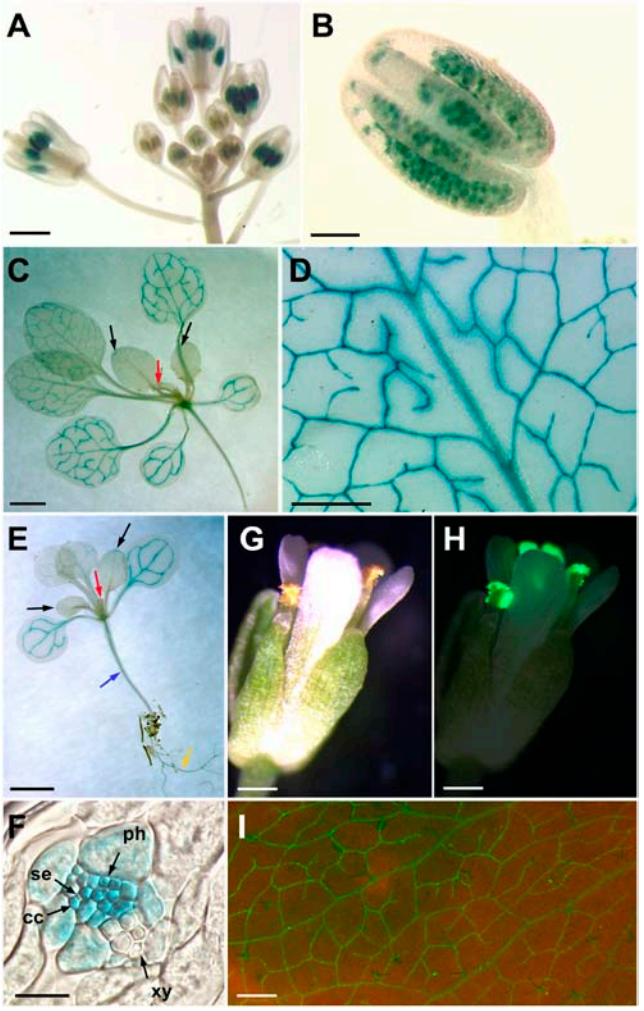

Figure 4. *GUS* and *GFP* reporter gene analyses of *AtINT4* expression. A, GUS-histochemical staining of an inflorescence from an *AtINT4* promoter-*GUS* plant showing GUS staining only in anthers. B, GUS-histochemical staining of an isolated anther from an *AtINT4* promoter-*GUS* plant showing GUS staining only in pollen grains. C, GUS-histochemical staining of the rosette of an *AtINT4* promoter-*GUS* plant showing GUS staining in the vascular strands of cotyledons and rosette leaves. Staining is absent from the youngest rosette leaf (red arrow), is strong in the older leaves of the rosette, and is visible only in the tips of the medium-sized leaves (transition leaves; black arrows). D, GUS-histochemical staining of a fully developed rosette leaf from an *AtINT4* promoter-*GUS* plant at higher magnification. GUS staining is restricted to the vascular strands and no staining is visible in the mesophyll. E, GUS-histochemical staining of a very young rosette of an *AtINT4* promoter-*GUS* plant showing GUS staining in the vascular strands of cotyledons. As in D, staining is absent from the youngest rosette leaf (red arrow) and is visible only in the tips of the medium-sized leaves (black arrows). Blue and yellow arrows show vascular GUS staining in the hypocotyl and roots. F, GUS-histochemical staining of a section through a minor vein of an *AtINT4* promoter-*GUS* leaf. Staining is seen only in the phloem part of the vein (xy, xylem; ph, phloem) and stronger in the companion cells (cc) than in the sieve elements (se). G, Flower of an *AtINT4* promoter-*GFP* plant photographed in white light. H, Same flower as in G under GFP excitation light. GFP fluorescence is restricted to pollen grains in the opened anthers, confirming the result obtained with *AtINT4* promoter-*GUS* plants in B. I, GFP fluorescence in the vascular tissue of a mature rosette leaf from an *AtINT4* promoter-*GFP* plant, confirming the result obtained with *AtINT4* promoter-*GUS* plants in D. Red color results from chlorophyll autofluorescence under GFP excitation light. Bars are 50 μm in F, 100 μm in B, 0.5 mm in G, H, and I, 1 mm in A and D, and 2 mm in C and E.

proceeded toward the petioles during leaf development. This expression pattern (pollen and vascular tissue) was observed in 22 of 24 analyzed *AtINT4* promoter-*GUS* plants and in 23 of 24 analyzed *AtINT4* promoter-*GFP* plants.

For further characterization of the precise tissue expressing *AtINT4* within the vascular tissue, we analyzed cross sections of *AtINT4* promoter-*GUS* leaves. Figure 4F shows a cross section through the midrib of a leaf from an *AtINT4* promoter-*GUS* plant, which shows that GUS staining is restricted to the phloem.

Immunohistochemical Analyses of AtINT4 Localization

Antisera were raised against the peptide NH_2-LLEVGFKPSILRRREKKGKEVDAA-COOH that corresponds to amino acids 559 to 582 at the very C terminus of AtINT4. This sequence was not found in any other Arabidopsis protein. The quality of the obtained sera was tested on detergent extracts from total membranes isolated from yeast strains ScLEX30 (harbors plasmid NEV-N [Sauer and Stolz, 2000] with *AtINT4* cDNA in sense orientation) and SSY9 (harbors the empty NEV-N vector). Figure 5A shows a western blot of these extracts after electrophoretic separation and incubation with three different antisera that had been raised in a guinea pig (αAtINT4-GP) or in two rabbits (αAtINT4-R1 and αAtINT4-R2). Labeled bands with an apparent molecular mass of about 55 kD and weaker signals of about 110 kD were detected with all sera in the *AtINT4*-expressing cells. These bands were absent in the extracts from SSY9 cells, indicating that the additional bands in ScLEX30 cells represent the monomeric form and the dimerized form of the AtINT4 protein.

The difference between the apparent molecular mass of the monomeric form (55 kD) and the molecular mass deduced from the DNA sequence (62.9 kD) was unexpected. Typically, lipophilic proteins run at higher apparent molecular masses on SDS gels, which results from excess binding of SDS (Beyreuther et al., 1980; Gahrtz et al., 1994; Barth et al., 2003). A reduced apparent molecular mass may result from protein modification (e.g. by proteolytic cleavage).

In a next step, the αAtINT4-GP antiserum that gave the best signals in Figure 5A was used to study the occurrence of AtINT4 protein in sections of Arabidopsis leaves and flowers by immunohistochemistry. Binding of antibody was visualized with an anti-guinea pig IgG-fluorescein isothiocyanate (FITC)-isomer 1-conjugate. In agreement with the strong expression of *AtINT4* in

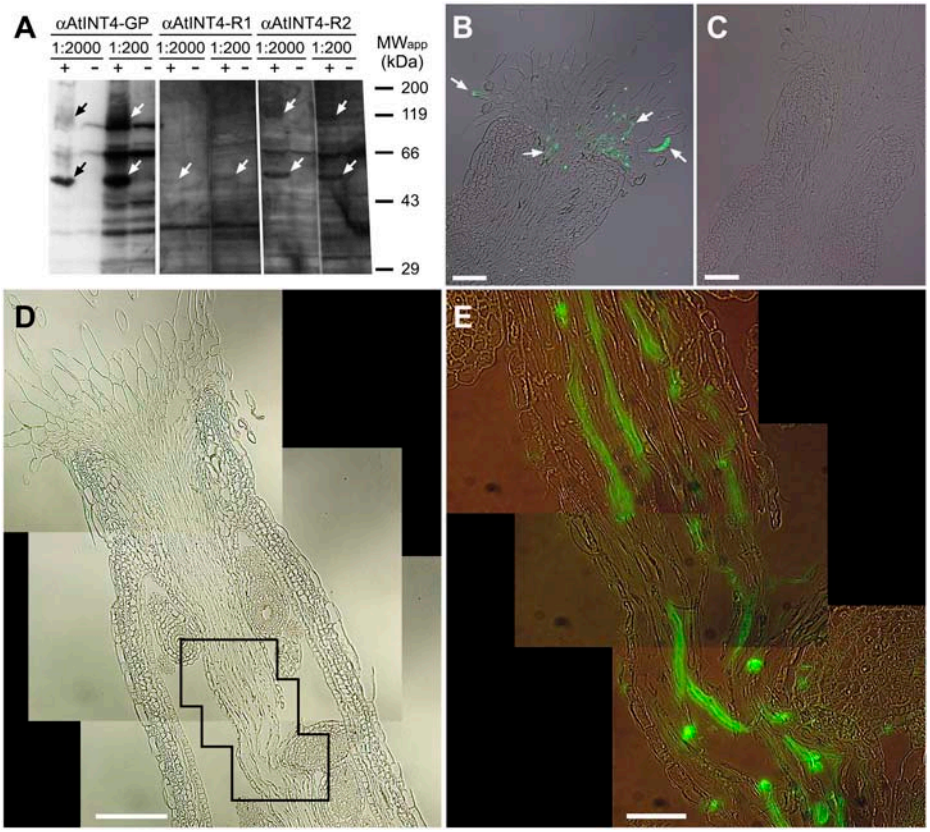

Figure 5. Immunohistochemical analyses of AtINT4 distribution in Arabidopsis wild-type plants. A, Antisera obtained from a guinea pig (αAtINT4-GP) or from two rabbits (αAtINT4-R1 and αAtINT4-R2) were analyzed at two different dilutions (1:200 and 1:2,000) on western blots of detergent extracts from total membrane preparations of yeast strains ScLEX30 (*AtINT4*-expressing strain; +) and SSY9 (control strain; −). All sera recognized additional protein bands of about 55 kD in strain ScLEX30 (arrows). The αAtINT4-GP and αAtINT4-R2 sera also recognized the dimeric form of the protein at about 110 kD (arrows). B, Longitudinal section through the style of a wild-type Arabidopsis plant that was treated with αAtINT4-GP (1:100) and anti-guinea pig second antibody (FITC-conjugated; 1:300). An overlay of the white-light picture and the fluorescence image is presented. Germinating pollen grains and growing pollen tubes are marked with arrows. C, Longitudinal section through the style of a wild-type Arabidopsis plant that was treated with guinea pig preimmune serum (1:100) and with anti-guinea pig second antibody (FITC-conjugated; 1:300). An overlay of the white-light picture and the fluorescence image is presented. D, Longitudinal section through the style and ovary of a wild-type Arabidopsis plant taken under white light. The boxed area marks the region that is shown at higher magnification in E. E, Longitudinal section through the style of a wild-type Arabidopsis plant that was treated with αAtINT4-GP (1:100) and with anti-guinea pig second antibody (FITC-conjugated; 1:300). An overlay of the white-light picture and the fluorescence image is presented. Bars are 50 μm in B and C, 100 μm in D, and 25 μm in E.

pollen (http://www.genevestigator.ethz.ch), we obtained strong signals in pollen grains and tubes that germinated or grew on Arabidopsis stylar papillae (Fig. 5B). These signals were absent in sections incubated with preimmune serum (Fig. 5C). Pollen tubes could also be labeled in the transmitting tissue on their way to the ovules (Fig. 5, D and E). Under no conditions were we able to detect αAtINT4-GP-dependent signals in leaves (data not shown). This might be due to the comparably low expression of *AtINT4* in the vasculature that is apparently too low to yield significant leaf-specific *AtINT4* expression on microarrays (Genevestigator: https:/www.genevestigator.ethz.ch).

In contrast to the GUS and GFP data (Fig. 4, B and H), no immunosignals were obtained in mature pollen grains that were still in the anthers. This suggests that the *AtINT4* promoter is active in these pollen grains to form *AtINT4* mRNA, but that this mRNA is translated only after hydration of the pollen on Arabidopsis stylar tissue.

Transient Expression of an *AtINT4-GFP* Construct

The subcellular localization of AtINT4 in planta was analyzed using an AtINT4 protein with GFP fused to its C terminus. To this end, the plasmid pSS24 that drives expression of the *AtINT4-GFP* fusion under the control of an enhanced 35S promoter was used for transient expression in Arabidopsis protoplasts (Fig. 6, A and B) or in particle-bombarded epidermis cells of tobacco (Fig. 6C). *AtINT4-GFP*-expressing cells and

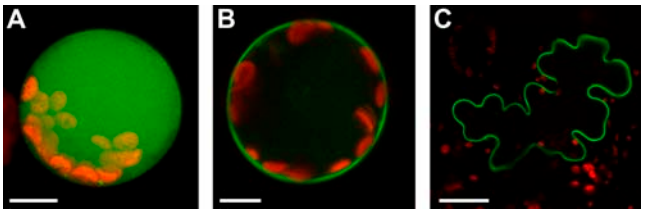

Figure 6. Analysis of subcellular localization of AtINT4 by transient expression of an *AtINT4-GFP* fusion. A, Maximal projection of confocal sections taken from an Arabidopsis protoplast expressing *AtINT4-GFP*. B, Single optical section from another *AtINT4-GFP*-expressing Arabidopsis protoplast shown in A. C, Transient expression of *AtINT4-GFP* in a tobacco epidermis cell from the same construct after particle bombardment of a detached tobacco leaf. Red fluorescence shows chlorophyll autofluorescence in A to C. Scale bars are 10 μm in A and B and 20 μm in C.

protoplasts were analyzed with a confocal microscope. In all analyses, the red autofluorescence of the chloroplasts was located inside the GFP-labeled structure (Fig. 6, A–C). No GFP fluorescence was found in any other structure inside the transformed cells, indicating that, in both plant expression systems (Arabidopsis and tobacco), the AtINT4-GFP fusion protein is located in the plasma membrane.

Analysis of Mutant Plants Harboring a T-DNA Insertion in the *AtINT4* Gene

Screening of publicly available libraries identified a mutant line (Salk_082661, Atint4-2) with a T-DNA insertion in the second exon of the *AtINT4* gene, 929 bp after the start ATG (Fig. 7A). We performed PCR reactions to identify homozygous Atint4-2 plants (e.g. plant 2 in the PCR shown in Fig. 7A) and used these plants for further analyses. Homozygous mutant plants showed a complete loss of intact *AtINT4* mRNA (Fig. 7B, i), whereas partial *AtINT4* mRNAs resulting from the sequences flanking the T-DNA insertion could be amplified from wild-type and Atint4-2 RNA preparations. The 840-bp fragment flanking the left border of the T-DNA insertion (Fig. 7B, 5′ end) is likely to result from AtINT4-promoter transcriptional activity. The 314-bp fragment flanking the predicted (but not sequenced) right border of the T-DNA insertion (Fig. 7B, 3′ end) most likely results from a promoter activity within the T-DNA insertion. Nevertheless, growth analyses under standard conditions (on soil in the growth chamber: 21°C, 60% relative humidity, long day [16-h light/8-h dark] or short day [8-h light/16-h dark]), on different concentrations of NaCl (10–100 mM), or on different concentrations of myoinositol in the growth medium (0–100 mM) revealed no phenotypic differences between the T-DNA insertion line and the isogenic wild type. Also, the fertility of the plants was not affected by the T-DNA insertion in *AtINT4*.

DISCUSSION

This article presents a detailed characterization of AtINT4 (At4g16480), a high-affinity, plasma membrane-localized H^+ symporter that is specific for myoinositol. AtINT4 represents one of four transporters (AtINT1–AtINT4) that form an independent subfamily within the MST-like superfamily in Arabidopsis that was named after the *AtSTP* gene family of plasma membrane-localized MSTs (Sauer et al., 1990; Büttner and Sauer, 2000).

So far, only members of the sugar transporter and the PLT subfamilies of the Arabidopsis MST-like superfamily were characterized by functional expression. Individual members of several other subfamilies have

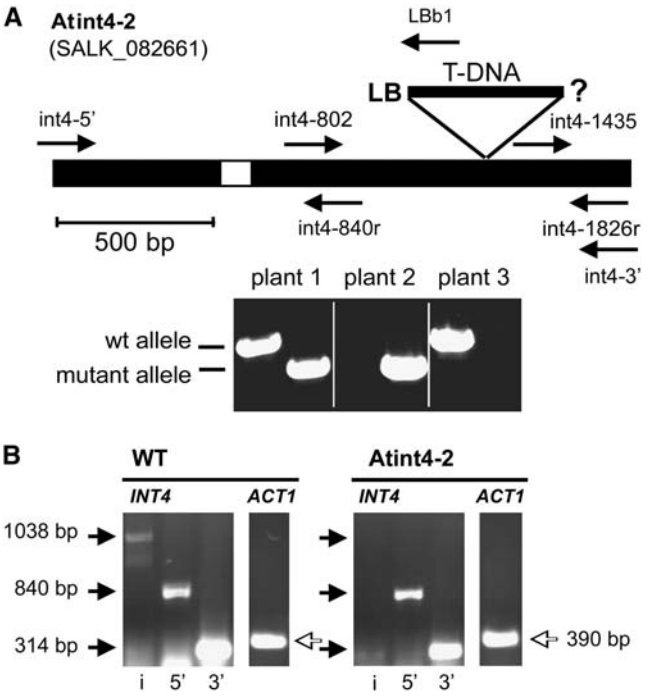

Figure 7. Characterization of the T-DNA insertion-line Atint4-2. A, Site of T-DNA in the second exon of the *AtINT4* gene in the SALK_082661 line (Atint4-2), the orientation of the insertion (the right border could not be determined), and the position of the primers that were used to identify wild-type and mutant alleles in Arabidopsis plants (int4-802 and int4-1826r) or *AtINT4* mRNAs in wild type and plants (shown in B). Examples of a heterozygous mutant (plant 1), a homozygous mutant (plant 2), and a wild-type (plant 3) plant are given. B, Identification of intact (i [primers: int4-802 and int4-3′ → 1,038 bp]) and partial (5′ = mRNA fragment upstream from the T-DNA insertion site [primers: int4-5′ and int4-840r → 840 bp]; 3′ = downstream from the T-DNA insertion site [primers: int4-1435 and int4-3′ → 314 bp]) *AtINT4* mRNAs in leaves from Arabidopsis wild-type and Atint4-2 mutant plants. Whereas the 1,038-bp fragment that results from intact *AtINT4* mRNA was amplified only from cDNA from wild-type leaves and absent in Atint4-2, *AtINT4* partial mRNAs from sequences flanking the T-DNA insertion (5′ and 3′ ends) were obtained both from wild-type and mutant RNA preparations. *ACT1* mRNA (control) was also amplified from wild-type and mutant plants. Contamination with genomic DNA (*ACT1* fragment would be 490 bp) was not detected.

been studied (At1g08930 [AtERD6], an early dehydration induced gene [Kiyosue et al., 1998]; At5g16150 [pGlcT], a putative plastidic transporter [Weber et al., 2000]; At5g27350 [AtSFP1], a senescence-induced gene [Quirino et al., 2001]), but functional analysis of the corresponding proteins failed.

AtINT4 Is a Plasma Membrane-Localized Transporter That Mediates H^+ Symport of Myoinositol

The functional characterization of AtINT4 is based on expression of its cDNA in bakers' yeast and Xenopus oocytes. In both systems, AtINT4 was characterized as a myoinositol transporter, in yeast by the complementation of a growth defect and in Xenopus by the analysis of currents elicited by this substrate. The latter analyses demonstrated that myoinositol is transported across the plasma membrane via an H^+-symport mechanism (Fig. 3).

These analyses suggested, and the localization of AtINT4-GFP in plasma membranes of Arabidopsis and tobacco fusion confirmed (Fig. 6), that the AtINT4 protein is a plasma membrane transporter. An H^+-dependent transport of myoinositol, the only identified substrate of AtINT4, has also been described for AtPLT5, another plasma membrane transporter of Arabidopsis (Klepek et al., 2005). However, AtPLT5 has a broad substrate specificity (pentoses, hexoses, linear polyols of various chain lengths, and cyclitols) and its $K_{m\text{-inositol}}$ (3.5 mM) is 15 times higher than the $K_{m\text{-inositol}}$ of AtINT4 (240 μM). Thus, AtINT4 is characterized as a high-specificity, high-affinity transporter for myoinositol, and myoinositol is likely to represent the physiological substrate of AtINT4. In contrast, it is not clear whether myoinositol plays an important role as a substrate for AtPLT5, which has much higher affinities for other substrates. More recent data suggest that the primary substrate of AtPLT5 and other members of the AtPLT family may be xylitol, which is transported by different AtPLTs with K_m values between 100 and 200 μM (Y.S. Klepek, M. Volke, and N. Sauer, unpublished data).

The only plant myoinositol transporters cloned so far were identified in the common ice plant (*MITR1* and *MITR2*; Chauhan et al., 2000). Using antisera that had been raised against MITR1-specific or MITR2-specific peptides, both transporters were localized to tonoplast membranes (Chauhan et al., 2000). MITR1 was described as a Na^+/myoinositol symporter and it was assumed that MITR2 would behave the same way (Chauhan et al., 2000).

In contrast, a myoinositol transporter from the protozoan *Leishmania donovani* (LdD1) and a human myoinositol transporter (HMIT) were both characterized as H^+ symporters by expression in Xenopus oocytes (Drew et al., 1995; Uldry et al., 2001). Also, two plasma membrane myoinositol transporters from bakers' yeast (ScITR1 and ScITR2) had been shown to be energy dependent and, although direct proof for an H^+-symport mechanism has not been presented, Na^+ has been excluded as a cotransported ion (Nikawa et al., 1991).

In addition to the H^+ symporter *HMIT* (Uldry et al., 2001), a Na^+/myoinositol symporter gene (*SMIT1*) has been cloned in mammals (Kwon et al., 1992). This SMIT1 protein shares significant homology with the well-characterized animal Na^+/Glc symporter SGLT1 (Hediger et al., 1987). It has been discussed (Uldry et al., 2001) that the side-by-side occurrence of H^+-dependent and Na^+-dependent myoinositol transporters in animals might be necessary to allow the energy-dependent transport of myoinositol also at low extracellular pH values, where HMIT is most active (Uldry et al., 2001) and SMIT is almost inactive (Matskevitch et al., 1998). Interestingly, all mammalian Na^+ symporters (including SMIT1) belong to one superfamily of transporters, which is called the SGLT family (Turk and Wright, 1997), whereas all H^+ symport/myoinositol transporters (LdD1, ScITR1, ScITR2, HMIT, and AtINT4) are members of the major facilitator superfamily (Marger and Saier, 1993). These two superfamilies of symporters are thought to have evolved primarily on the basis of the different cotransported ions (Pajor and Wright, 1992). If this is true, it is quite unlikely that MITR1 and MITR2 represent Na^+ symporters within a family of H^+ symporters and uniporters.

The report that MITR1 and MITR2 act as Na^+ symporters (Chauhan et al., 2000) was not based on functional analyses. Rather, it was an interpretation of *MITR1* transcript levels and growth rates of complemented yeast cells. A direct study of myoinositol transport has neither been performed in yeast nor in Xenopus oocytes. Moreover, the described growth-promoting effect of MITR1 in complemented yeast cells (Chauhan et al., 2000) is also observed in yeast cells complemented with the H^+ symporter AtINT4 (Fig. 2). This observation must, therefore, have a reason that is independent from the postulated Na^+-symport mechanism. An explanation might be that the recombinant plant myoinositol transporter enables the complemented yeast cells to accumulate myoinositol as an osmolyte and thus to grow better at increased concentrations of NaCl.

Using antisera that had been raised against peptides from the central cytoplasmic loop, MITR1 and MITR2 were detected in vacuolar membrane fractions (Chauhan et al., 2000). Surprisingly, AtINT4, which is the closest relative of the four Arabidopsis AtINT proteins, was now localized to the plasma membrane (this article). In a few cases, where members of the same transporter family were found in the tonoplast or in the plasma membrane so far (e.g. the aquaporins), the protein sequences allow discrimination between tonoplast intrinsic proteins and plasma membrane intrinsic proteins and predictions can even be made for proteins encoded by newly cloned cDNAs (Kjellbom et al., 1999; Borstlap, 2002). This seems to be different for plant inositol transporters. An alternative explanation is, however, that the used antibodies (Chauhan et al.,

2000) were not as specific as predicted. This may occur whether the ice plant *MITR* family has more than the two genes that have so far been identified or whether another, so far unknown ice plant transporter, possesses a similar antigenic domain.

AtINT4 Is Expressed in Pollen and in the Vasculature

AtINT4 expression was observed in pollen grains and in the vascular tissue of *AtINT4* promoter-*GUS* and *AtINT4* promoter-*GFP* plants (Fig. 4). The expression of *AtINT4* in pollen, but not in the vasculature, had been predicted from microarray analyses (https://www.genevestigator.ethz.ch). From Figure 4, D and I, it is obvious that gene expression in the vasculature of Arabidopsis leaves is limited to very few cells in a leaf. Moreover, analyses of *AtINT4* promoter-*GFP* plants (Fig. 4, H and I) suggest that the relative expression of *AtINT4* is stronger in pollen than in the vasculature. Together, these observations explain why vascular expression has not been seen in microarray analyses.

Attempts to confirm these expression data by immunohistochemical analyses were successful for pollen tubes. Sections through Arabidopsis stylar tissue showed FITC-dependent fluorescence only after incubation with an αAtINT4 antiserum as the first antiserum (Fig. 5B) and not with preimmune serum (Fig. 5C). AtINT4 was also immunodetected in pollen tubes growing in the transmitting tissue (Fig. 5D). Unexpectedly, however, no signals were seen in pollen grains that were still in the anthers (data not shown), although *AtINT4* promoter activity in mature pollen was demonstrated by reporter gene analyses in Figure 4.

Similar observations (i.e. translation of a preformed mRNA only after hydration and germination of pollen on the stylar tissue) have also been made for other genes (Linskens et al., 1970; Lin et al., 1987; Capkova et al., 1988; Stadler et al., 1999). It has been postulated that this mechanism enables rapid pollen germination and a high rate of pollen tube growth, primary factors governing the competition between pollen in reaching and effecting fertilization (Mascarenhas, 1990). However, homozygous Atint4-2 T-DNA insertion plants do form a normal number of fertile seeds, suggesting that the growth rate and the fertility of Atint4-2 pollen is not significantly reduced, at least under greenhouse and growth chamber conditions.

The Physiological Role of AtINT4 Remains to Be Elucidated

With several sets of PCR primers it was not possible to identify a complete *AtINT4* mRNA in Atint4-2 plants (Fig. 7; data not shown). Nevertheless, these plants do form fertile seeds and all other parameters analyzed (standard growth conditions, salinity stress, and varying inositol concentrations) did not differ from isogenic wild-type plants. Identification of *AtINT4* mRNA fragments that correspond to *AtINT4* genomic sequences flanking both sides of the T-DNA insertion raises the question of whether the encoded, truncated transporter fragments can form a functional unit. In principle, this cannot be excluded because it has been shown for other transporters that truncated proteins encoded by split mRNAs can form a functional complex (Wrubel et al., 1990; Reinders et al., 2002).

It has been reported that Arabidopsis transports small amounts of raffinose in its phloem (Haritatos et al., 2000) and it is known that raffinose is synthesized by the enzyme galactinol synthase from UDP-Gal and myoinositol (Kandler and Hopf, 1982). In fact, the source leaf-specific expression of *AtINT4* resembles the expression pattern described for *AtSUC2* (Truernit and Sauer, 1995) and suggests a role for AtINT4 in phloem loading. Activity of the myoinositol transporter AtINT4 in companion cells might be necessary to deliver mesophyll-derived myoinositol to the companion cells or for retrieving companion cell-synthesized myoinositol that has been lost in the apoplast.

Analyses of *AtGolS1* promoter-*GUS* plants (Panikulangara et al., 2004) had demonstrated that the Arabidopsis galactinol synthase gene (*AtGolS1*) is expressed in all vegetative tissues, with enhanced levels in the vascular tissue. We speculated that myoinositol might be used by AtGolS1 in companion cells for raffinose synthesis. In several analyses, the concentrations of myoinositol and raffinose were determined in Atint4-2 plants and in the isogenic Arabidopsis wild type by ion chromatography (data not shown). Myoinositol concentrations varied between 0.90 ± 0.22 nmol mg^{-1} fresh weight ($n = 8$) in rosette leaves from wild-type plants and 0.88 ± 0.25 nmol mg^{-1} fresh weight ($n = 9$) in rosette leaves from *AtINT4* T-DNA insertion plants, indicating that the concentration of myoinositol in whole leaves was not affected in Atint4-2 plants. The concentrations of raffinose, however, were too low (between 0.05−0.2 nmol mg^{-1} fresh weight) and too variable to show significant and reproducible concentration differences. Some experiments suggested such a difference, but in others the concentrations were more or less identical. The physiological role of raffinose transport in Arabidopsis is not really understood and a visible effect in the phenotype of plants with reduced raffinose synthesis might not be expected.

In ice plants, myoinositol transport is thought to play a role in salt tolerance. In Arabidopsis, there is no indication for a regulation of *AtINT4* expression by salt treatment (https://www.genevestigator.ethz.ch) nor is myoinositol accumulating in salt-grown Arabidopsis plants. Thus, AtINT4 does not seem to play a role in the response of Arabidopsis plants to salt treatment. Similarly, changes in the concentrations of exogenously supplied myoinositol (0 mM, 1 mM, 10 mM, and 100 mM) did not result in phenotypic differences between wild-type and Atint4-2 plants.

As for many other transporter genes, the roles of specific transport activity in pollen, pollen tubes, and phloem is still unclear. For a final answer to this

question, we will need double, triple, or quadruple knockout lines that are not yet available at this time.

MATERIALS AND METHODS

Strains and Growth Conditions

Arabidopsis (*Arabidopsis thaliana*) plants were grown in a growth chamber on potting soil under a 16-h light/8-h dark regime at 22°C and 60% relative humidity or in a greenhouse under ambient conditions. For heterologous expression of *AtINT4* cDNAs in yeast (*Saccharomyces cerevisiae*), we used strain D458-1B (Nikawa et al., 1991) or strain SEY2102 (Emr et al., 1983). *Escherichia coli* strain DH5α (Hanahan, 1983) was used for all basic cloning steps; fusion proteins for antisera were expressed in *E. coli* strain Rosetta (Novagen). Transformation of Arabidopsis was performed using *Agrobacterium tumefaciens* strain GV3101 (Holsters et al., 1980).

cDNA Cloning and Constructs for Yeast Expression

cDNAs of three of four Arabidopsis *AtINT* genes were amplified from total RNA isolated from Arabidopsis ecotype Columbia with gene-specific primers binding to the very 5′ ends (including the start ATG) or the very 3′ ends (including the stop codon) of the cDNAs. *Not*I cloning sites were introduced at both ends of *AtINT1* and *AtINT2*, and *Eco*RI cloning sites were introduced at both ends of *AtINT4*. The resulting cDNAs were digested with the respective enzymes, cloned into the yeast expression vectors NEV-E or NEV-N (Sauer and Stolz, 1994), and sequenced (pLEX114s = AtINT4 cDNA in NEV-E in sense orientation). The *AtINT4*-containing plasmids were used for transformation of yeast cells (Gietz et al., 1992). If not otherwise indicated, uptake experiments were performed in 50 mM sodium phosphate buffer (pH 5.0) as described (Sauer et al., 1990).

Heterologous Expression in *Xenopus laevis* Oocytes

For functional analysis in *Xenopus laevis* oocytes, the *AtINT4* insert of pLEX114s was excised with *Eco*RI and cloned into the plasmid pDK148 (Jespersen et al., 2002). *AtINT4* cRNA was prepared using the T7 mESSAGE mMACHINE RNA transcription kit (Ambion). Oocyte preparation and cRNA injection have been described elsewhere (Becker et al., 1996). In two-electrode voltage-clamp studies, oocytes were perfused with a standard solution containing 30 mM KCl, 65 mM NaCl, 1.5 mM $MgCl_2$, 1 mM $CaCl_2$, and were adjusted with MES/Tris buffers to pH values from 5.5 to 8.5. Substrate concentrations and pH values are indicated in the figures and figure legends. Currents in the absence of substrates were subtracted for leak correction.

AtINT4 Promoter-*GUS* and *AtINT4* Promoter-*GFP* Constructs and Plant Transformation

A 1,518-bp promoter *AtINT4* promoter fragment was PCR amplified from genomic DNA (Arabidopsis ecotype Columbia) using the primers INT4-p5 (5′-GTCCGAAAAAGCTTGGGTTCAAATCCCACTCTTGACA-3′) and INT4-p3 (5′-TCCTTCCACCATGGTTTCTTCTTGTCTGATCTCTC-3′). The primers introduced an N-terminal *Hin*dIII and a C-terminal *Nco*I site that were used to clone the resulting fragment in front of the ORF of *GFP* and a transcriptional terminator in a pUC19-based plasmid (pEPS1/pUC19; Imlau et al., 1999). The fragment was sequenced and the *AtINT4* promoter-*GFP* terminator box was cloned into pGPTV-BAR (Becker et al., 1992), yielding the plasmid pLEX164 (*AtINT4* promoter *GFP*), which was used for transformation of Arabidopsis (Clough and Bent, 1998). The plasmid pLEX110 (*AtINT4* promoter *GUS*) was also generated in pGPTV-BAR using the same promoter fragment.

Transient Expression of *AtINT4-GFP*

For transient expression of *AtINT4-GFP* fusions, we used the plasmid pSO35e (Klepek et al., 2005). The *AtINT4* coding sequence was PCR amplified using the primers AtINT4-*Nco*I-5 (5′-CCATGGTGGAAGGAGGAATTG-3′) and AtINT4-*Nco*I-3 (5′-CCATGGCAGCAGCATCGACTTCTTTGC-3′). These primers introduced *Nco*I sites at the start and at the very end of the *AtINT4* ORF, thereby replacing the stop codon of the original *AtINT4* sequence. This modified *AtINT4* ORF was inserted into the unique *Nco*I cloning site representing the start ATG of the *GFP* ORF in the pSO35e plasmid. The continuous ORF was confirmed by sequencing. The resulting plasmid was named pSS24.

pSS24 was used for transient expression of AtINT4 in Arabidopsis protoplasts (polyethylene glycol transformation; modified after Abel and Theologis [1994]) or in tobacco (*Nicotiana tabacum*) epidermis cells (particle bombardment; Klepek et al., 2005).

Analysis of the T-DNA Insertion Line *Atint4-2*

The T-DNA insertion line *Atint4-2* (Salk_082661) was identified using the Salk Institute T-DNA express gene-mapping tool (Alonso et al., 2003). Homozygous plants were identified in PCR reactions performed with genomic DNA and the primers int4-802 (5′-GGAGATGGAAGCTTTGAAACT-3′) and int4-1826r (5′-GACTTCTTTGCCCTTCTTCTC-3′) in combination with the primer LBb1 (5′-GCGTGGACCGCTTGCTGCAAC-3′) that binds near the left border within the T-DNA insertion (primer positions are shown in Fig. 7).

The primers int4-5′ (5′-ATATCTCTGAATTCAACAATGGTGGAAGGAGGAATTGCG-3′), int4-3′ (5′-ATATCTCTGAATTCTTAAGCAGCATCGACTTCTTTGCCC-3′), int4-840r (5′-AGCAGCGAGTCCACGTCGAAC-3′), and int4-1435 (5′-CCGTGGATCGTCAACTCT-3′) were used for reverse transcription-PCRs with total RNA from wild-type and mutant Arabidopsis leaves. The primers AtACT5 (5′-GCGATGAAGCTCAATCCAAACGAG-3′) and AtACT3 (5′-GGTCACGACCAGCAAGATCAAGAC-3′) were used to amplify the *AtACT1* mRNA.

Immunohistochemical Techniques and Western-Blot Analyses

For production of anti-AtINT4 antisera (αAtINT4), two oligonucleotides were annealed and cloned into the *Eco*RI/*Hin*dIII-digested vector pMAL-c2 (New England Biolabs), yielding the plasmid pSS11-AK4. The oligonucleotides encoded the C-terminal 24 amino acids of AtINT4 (LLEVGFKPSL LRRREKKGKEVDAA). The plasmid pSS11-AK4 was used to express a fusion of this peptide to the maltose-binding protein in *E. coli* strain Rosetta (Novagen). Expression of the protein was induced with isopropyl thiogalactoside, solubilized proteins were separated on polyacrylamide gels (Laemmli, 1970), bands were excised, and proteins were extracted and lyophilized. Antisera were generated by Pineda-Antikörper-Service.

Binding of anti-AtINT4 (αAtINT4) antibodies to microtome sections was visualized by treatment with anti-guinea pig IgG-FITC-isomer 1-conjugate (Sigma-Aldrich). Finally, microscopic slides were mounted in antifading medium (ProLong antifade kit; Molecular Probes) and viewed under appropriate excitation light.

Protein extracts of total membrane fractions from bakers' yeast were prepared as described (Sauer and Stolz, 2000), separated on SDS polyacrylamide gels (Laemmli, 1970), and transferred to nitrocellulose filters (Dunn, 1986). AtINT4 protein bands were detected by treatment of the filters with anti-rabbit or anti-guinea pig IgG-peroxidase conjugate (diluted 1:4,000 in blocking buffer) followed by incubation with Lumi-Light western-blotting substrate (Roche Diagnostics GmbH).

Ion Chromatography

To measure the concentrations of sugars and sugar alcohols, a BioLC DX600 system (Dionex) was used, including a gradient pump (GP50), a degasser module, an autosampler (AS50), and a pulsed amperometric detector (EG50). Separation of the anionic compounds was carried out using a CarboPack MA1 column (4 × 250 mm) connected to a guard column of the same material (4 × 10 mm) and an ATC-1 anion trap column, which was placed between the eluent and separation columns to remove the anionic contaminants present in the eluents. A linear gradient was accomplished with purest water (buffer A; Millipore) and 480 mM sodium hydroxide (Baker; 50% solution, buffer B). The column was equilibrated at a flow rate of 0.4 mL/min. The duration of the run was 65 min. The calibration and quantitative calculation of inositol and raffinose were carried out using chromeleon software 6.6.

Epifluorescence Microscopy and Detection of GFP Fluorescence

Images of GFP fluorescence were made with an epifluorescence microscope (Zeiss Axioskop; Carl Zeiss GmbH), with stereomicroscopes (Zeiss SV11 or Leica MZFLIII; Leica Microsystems) with an excitation wavelength of 460 to 500 nm or with a confocal laser-scanning microscope (Leica TCS SPII). Confocal images were processed using Leica confocal software 2.5. Emitted fluorescence was monitored at detection wavelengths longer than 510 nm.

ACKNOWLEDGMENTS

We thank Ruth Stadler for experimental help and Angelika Wolf for growing the Arabidopsis plants.

Received January 13, 2006; revised March 31, 2006; accepted March 31, 2006; published April 7, 2006.

LITERATURE CITED

Abel S, Theologis A (1994) Transient transformation of Arabidopsis leaf protoplasts: a versatile experimental system to study gene expression. Plant J **5:** 421–427

Alonso JM, Stepanova AN, Leisse TJ, Kim CJ, Chen H, Shinn P, Stevenson DK, Zimmerman J, Barajas P, Cheuk R, et al (2003) Genome-wide insertional mutagenesis of *Arabidopsis thaliana*. Science **301:** 653–657

Aoshima H, Yamada M, Sauer N, Komor E, Schobert C (1993) Heterologous expression of the H^+/hexose cotransporter from *Chlorella* in *Xenopus* oocytes and its characterization with respect to sugar specificity, pH and membrane potential. J Plant Physiol **141:** 293–297

Barth I, Meyer S, Sauer N (2003) PmSUC3: characterization of a SUT2/SUC3-type sucrose transporter from *Plantago major*. Plant Cell **15:** 1375–1385

Becker D, Dreyer I, Hoth S, Reid JD, Busch H, Lehnen M, Palme K, Hedrich R (1996) Changes in voltage activation, Cs^+ sensitivity, and ion permeability in H5 mutants of the plant K^+ channel KAT1. Proc Natl Acad Sci USA **93:** 8123–8128

Becker D, Kemper E, Schell J, Masterson R (1992) New plant binary vectors with selectable markers located proximal to the left T-DNA border. Plant Mol Biol **20:** 1195–1197

Beyreuther K, Bieseler B, Ehring R, Griesser H-W, Mieschendahl M, Müller-Hill B, Triesch I (1980) Investigation of structure and function of lactose permease of *Escherichia coli*. Biochem Soc Trans **8:** 675–676

Boorer KJ, Loo DD, Frommer WB, Wright EM (1996) Transport mechanism of the cloned potato H^+/sucrose cotransporter StSUT1. J Biol Chem **271:** 25139–25144

Borstlap AC (2002) Early diversification of plant aquaporins. Trends Plant Sci **7:** 529–530

Büttner M, Sauer N (2000) Monosaccharide transporters in plants: structure, function and physiology. Biochim Biophys Acta **1465:** 263–274

Capkova V, Hrabetova E, Tupy J (1988) Protein synthesis in pollen tubes: preferential formation of new species independent of transcription. Sex Plant Reprod **1:** 150–155

Chauhan S, Forsthoefel N, Ran Y, Quigley F, Nelson DE, Bohnert HJ (2000) Na^+/myoinositol symporters and Na^+/H^+-antiport in *Mesembryanthemum crystallinum*. Plant J **24:** 511–522

Clough SJ, Bent AF (1998) Floral dip: a simplified method for *Agrobacterium*-mediated transformation of *Arabidopsis thaliana*. Plant J **16:** 735–743

Drew ME, Langford CK, Klamo EM, Russell DG, Kavanaugh MP, Landfear SM (1995) Functional expression of a myoinositol/H^+ symporter from *Leishmania donovani*. Mol Cell Biol **15:** 5508–5515

Dunn SD (1986) Effects of the modification of transfer buffer composition on the renaturation of proteins in gels on the recognition of proteins on Western blots by monoclonal antibodies. Anal Biochem **157:** 144–153

Emr SD, Scheckman R, Flessel MC, Thorner J (1983) An MFα1-SUC2 (σ-factor-invertase) gene fusion for study of protein localisation and gene expression in yeast. Proc Natl Acad Sci USA **80:** 7080–7084

Gahrtz M, Stolz J, Sauer N (1994) A phloem specific sucrose-H^+ symporter from *Plantago major* L. supports the model of apoplastic phloem loading. Plant J **6:** 697–706

Gao Z, Maurousset L, Lemoine R, Yoo SD, Van Nocker S, Loescher W (2003) Cloning, expression, and characterization of sorbitol transporters from developing sour cherry fruit and leaf sink tissues. Plant Physiol **131:** 1566–1575

Gietz D, Jean WS, Woods RA, Schiestl RH (1992) Improved method for high efficiency transformation of intact yeast cells. Nucleic Acids Res **20:** 1425

Hanahan D (1983) Studies on transformation of *E. coli* with plasmids. J Mol Biol **166:** 557–580

Haritatos E, Medville RA, Turgeon R (2000) Minor vein structure and sugar transport in *Arabidopsis thaliana*. Planta **211:** 105–111

Hediger MA, Ikeda T, Coady M, Gundersen CB, Wright EM (1987) Expression of size-selected mRNA encoding the intestinal Na^+/glucose cotransporter in *Xenopus laevis* oocytes. Proc Natl Acad Sci USA **84:** 2634–2637

Holsters M, Silva B, Van Vliet F, Genetello C, De Block M, Dhaese P, Depicker A, Inze D, Engler G, Villarroel R, et al (1980) The functional organization of the nopaline *Agrobacterium tumefaciens* plasmid pTiC58. Plasmid **3:** 212–230

Imlau A, Truernit E, Sauer N (1999) Cell-to-cell and long-distance trafficking of the green fluorescent protein in the phloem and symplastic unloading of the protein into sink tissues. Plant Cell **11:** 309–322

Jespersen T, Grunnet M, Angelo K, Klaerke DA, Olesen SP (2002) Dual-function vector for protein expression in both mammalian cells and *Xenopus laevis* oocytes. Biotechniques **32:** 536–540

Kandler O, Hopf H (1982) Oligosaccharides based on Suc (sucrosyl oligosaccharides). *In* FA Loewus, W Tanner, eds, Plant Carbohydrates 1. Encyclopedia of Plant Physiology: Plant Carbohydrates I, Intracellular Carbohydrates, New Series, Vol 13 A. Springer-Verlag, Berlin, pp 348–383

Kanter U, Usadel B, Guerineau F, Li Y, Pauly M, Tenhaken R (2005) The inositol oxygenase gene family of *Arabidopsis* is involved in the biosynthesis of nucleotide sugar precursors for cell-wall matrix polysaccharides. Planta **221:** 243–254

Kiyosue T, Abe H, Yamaguchi-Shinozaki K, Shinozaki K (1998) ERD6, a cDNA clone for an early dehydration-induced gene of *Arabidopsis*, encodes a putative sugar transporter. Biochim Biophys Acta **1370:** 187–191

Kjellbom P, Larsson C, Johansson II, Karlsson M, Johanson U (1999) Aquaporins and water homeostasis in plants. Trends Plant Sci **4:** 308–314

Klepek YS, Geiger D, Stadler R, Klebl F, Landouar-Arsivaud L, Lemoine R, Hedrich R, Sauer N (2005) *Arabidopsis* POLYOL TRANSPORTER5, a new member of the monosaccharide transporter-like superfamily, mediates H^+-symport of numerous substrates, including *myo*-inositol, glycerol, and ribose. Plant Cell **17:** 204–218

Kwon HM, Yamauchi A, Uchida S, Preston AS, Garcia-Perez A, Burg MB, Handler JS (1992) Cloning of the cDNA for a Na^+/*myo*-inositol cotransporter, a hypertonicity stress protein. J Biol Chem **267:** 6297–6301

Laemmli UK (1970) Cleavage of structural proteins during the assembly of the head of bacteriophage T4. Nature **227:** 680–685

Lehle L (1990) Phosphatidyl inositol metabolism and its role in signal transduction in growing plants. Plant Mol Biol **15:** 647–658

Lin J-J, Dickinson DB, Ho T-HD (1987) Phytic acid metabolism in lily (*Lilium longiflorum* Thunb.) pollen. Plant Physiol **83:** 408–413

Linskens HF, Schrauwen JAM, Konings RNK (1970) Cell-free protein synthesis with polysomes from germinating *Petunia* pollen grains. Planta **90:** 153–162

Loewus FA, Murthy PPN (2000) *myo*-Inositol metabolism in plants. Plant Sci **150:** 1–19

Lorence A, Chevone BI, Mendes P, Nessler CL (2004) *myo*-Inositol oxygenase offers a possible entry point into plant ascorbate biosynthesis. Plant Physiol **134:** 1200–1205

Marger MD, Saier MH Jr (1993) A major superfamily of transmembrane facilitators that catalyze uniport, symport and antiport. Trends Biochem Sci **18:** 13–20

Mascarenhas JP (1990) Gene activity during pollen development. Annu Rev Plant Physiol Plant Mol Biol **41:** 317–338

Matskevitch J, Wagner CA, Risler T, Kwon HM, Handler JS, Waldegger S, Busch AE, Lang F (1998) Effect of extracellular pH on the *myo*-inositol transporter SMIT expressed in *Xenopus* oocytes. Pflugers Arch **436:** 854–857

Nelson DE, Koukoumanos M, Bohnert HJ (1999) *Myo*-inositol-dependent sodium uptake in ice plant. Plant Physiol **119:** 165–172

Nelson DE, Rammesmayer G, Bohnert HJ (1998) Regulation of cell-specific inositol metabolism and transport in plant salinity tolerance. Plant Cell **10:** 753–764

Nikawa J, Tskugoshi Y, Yamashita S (1991) Isolation and characterization of two distinct *myo*-inositol transporter genes of *Saccharomyces cerevisiae*. J Biol Chem **266:** 11184–11191

Noiraud N, Maurousset L, Lemoine R (2001) Identification of a mannitol transporter, AgMaT1, in celery phloem. Plant Cell **13:** 695–705

Page RDM (1996) TREEVIEW: an application to display phylogenetic trees on personal computers. Comput Appl Biosci **12:** 357–358

Pajor AM, Wright EM (1992) Cloning and functional expression of a mammalian Na^+/nucleoside cotransporter: a member of the SGLT family. J Biol Chem **267:** 3557–3560

Panikulangara TJ, Eggers-Schumacher G, Wunderlich M, Stransky H, Schöffl F (2004) Galactinol synthase1: a novel heat shock factor target gene responsible for heat-induced synthesis of raffinose family oligosaccharides in Arabidopsis. Plant Physiol **136:** 3148–3158

Quirino BF, Reiter WD, Amasino RD (2001) One of two tandem *Arabidopsis* genes homologous to monosaccharide transporters is senescence-associated. Plant Mol Biol **46:** 447–457

Raboy V (2003) *myo*-Inositol-1,2,3,4,5,6-hexakisphosphate. Phytochemistry **64:** 1033–1043

Ramsperger-Gleixner M, Geiger D, Hedrich R, Sauer N (2004) Differential expression of sucrose transporter and polyol transporter genes during maturation of common plantain companion cells. Plant Physiol **134:** 147–160

Reinders A, Panshyshyn JA, Ward JM (2005) Analysis of transport activity of *Arabidopsis* sugar alcohol permease homolog AtPLT5. J Biol Chem **280:** 1594–1602

Reinders A, Schulze W, Thaminy S, Stagljar I, Frommer WB, Ward JM (2002) Intra- and intermolecular interactions in sucrose transporters at the plasma membrane detected by the split-ubiquitin system and functional assays. Structure **10:** 763–772

Robinson KS, Lai K, Cannon TA, McGraw P (1996) Inositol transport in *Saccharomyces cerevisiae* is regulated by transcriptional and degradative endocytic mechanisms during the growth cycle that are distinct from inositol-induced regulation. Mol Biol Cell **7:** 81–89

Sauer N, Friedländer K, Gräml-Wicke U (1990) Primary structure, genomic organization and heterologous expression of a glucose transporter from *Arabidopsis thaliana*. EMBO J **9:** 3045–3050

Sauer N, Stolz J (1994) SUC1 and SUC2: two sucrose transporters from *Arabidopsis thaliana*; expression and characterization in bakers' yeast and identification of the histidine tagged protein. Plant J **6:** 67–77

Sauer N, Stolz J (2000) Expression of foreign transport proteins in yeast. *In* SA Baldwin, ed, Practical Approach Series. Oxford University Press, New York, pp 79–105

Schultz C, Gilson P, Oxley D, Youl J, Bacic A (1998) GPI-anchors on arabinogalactan-proteins: implications for signalling in plants. Trends Plant Sci **3:** 426–431

Sheveleva E, Chmara W, Bohnert HJ, Jensen RG (1997) Increased salt and drought tolerance by D-ononitol production in transgenic *Nicotiana tabacum*. Plant Physiol **115:** 1211–1219

Shi J, Wang H, Hazebroek J, Ertl DS, Harp T (2005) The maize low-phytic acid 3 encodes a *myo*-inositol kinase that plays a role in phytic acid biosynthesis in developing seeds. Plant J **42:** 708–719

Stadler R, Truernit E, Gahrtz M, Sauer N (1999) The AtSUC1 sucrose carrier may represent the osmotic driving force for anther dehiscence and pollen tube growth in *Arabidopsis*. Plant J **19:** 269–278

Taji T, Ohsumi C, Iuchi S, Seki M, Kasuga M, Kobayashi M, Yamaguchi-Shinozaki K, Shinozaki K (2002) Important roles of drought- and cold-inducible genes for galactinol synthase in stress tolerance in *Arabidopsis thaliana*. Plant J **29:** 417–426

Thomas JC, Bohnert HJ (1993) Salt stress perception and plant growth regulators in the halophyte *Mesembryanthemum crystallinum*. Plant Physiol **103:** 1299–1304

Thompson JD, Gibson TJ, Plewniak F, Jeanmougin F, Higgins DG (1997) The ClustalX windows interface: flexible strategies for multiple sequence alignment aided by quality analysis tools. Nucleic Acids Res **24:** 4876–4882

Truernit E, Sauer N (1995) The promoter of the *Arabidopsis thaliana SUC2* sucrose-H^+ symporter gene directs expression of β-glucuronidase to the phloem: evidence for phloem loading and unloading by SUC2. Planta **196:** 564–570

Turk E, Wright EM (1997) Membrane topology motifs in the SGLT cotransporter family. J Membr Biol **159:** 1–20

Uldry M, Ibberson M, Horisberger JD, Chatton JY, Riederer BM, Thorens B (2001) Identification of a mammalian H^+-*myo*-inositol symporter expressed predominantly in the brain. EMBO J **20:** 4467–4477

Watari J, Kobae Y, Yamaki S, Yamada K, Toyofuku K, Tabuchi T, Shiratake K (2004) Identification of sorbitol transporters expressed in the phloem of apple source leaves. Plant Cell Physiol **45:** 1032–1041

Weber A, Servaites JC, Geiger DR, Kofler H, Hille D, Groner F, Hebbeker U, Flügge UI (2000) Identification, purification, and molecular cloning of a putative plastidic glucose translocator. Plant Cell **12:** 787–802

Wrubel W, Stochaj U, Sonnewald U, Theres C, Ehring R (1990) Reconstitution of an active lactose carrier in vivo by simultaneous synthesis of two complementary protein fragments. J Bacteriol **172:** 5374–5381